www.sensorsportal.com

Sensors & Transducers

http://www.sensorsportal.com

An Investigation on Test Signal Transmission at Temperature Changing Environment

[1] Men Xiuhua, [1] Shao Haiyan, [2] Liu Baojian, [1] Li Yingjun, [1] Fu Xiuli
[1] School of Mechanical Engineering, University of Jinan, Jinan, 250022, China
[2] Saic-Iveco Hongyan Commercial Vehicle Co. Ltd, Chongqing, 401122, China
[1] Tel.: +8615562516593
E-mail: me_menxh@ujn.edu.cn

Received: 20 May 2013 /Accepted: 12 August 2013 /Published: 20 August 2013

Abstract: In vibration test, the signal transmission is affected significantly by high ambient temperature. The basis of on traditional transmission theory, the telegraph operator equation is satisfied for analyzing signal feature. When ambient temperature increases from low to high, transmission parameters RLCG change correspondingly. Considering circuit feature of signal transmission, Kirchhoff's Law is applied to establish a discrete temperature-time signal transmission model. And the FDTD method is applied to give a new iterative algorithm for achieving the solution of voltage u\and current. The signal transmissions with different temperature changing process are realized using above simulation. The results show that the amplitude of output signal is gradually attenuate with the rise of conductor temperature. Compared with amplitude at 30 °C, the attenuate degree comes to 10 % at 300 °C. The amplitude attenuation is more evident due to the coexistence of temperature rise and drop. The corresponding experiment has been conducted and the results can meet that of proposed model. It provides a new method for improving the accuracy of vibration test signal.

Keywords: Vibration test, Signal transmission, Temperature changing environment, FDTD, Temperature gradient, Signal amplitude.

1. Introduction

The test signal processing and analysis are the key component of the power generating machine test system. Many effective methods have been proposed to improve the accuracy of signal analysis [1]. In fact, it is not enough for analyzing signal feature only using above processing technique. The change of ambient temperature also takes important effect on signal transmission path [2], which would ultimately change the original features of test signal. Thus, to obtain exact feature of signal, it is significant to study on changing characteristics of test signal transmission in temperature-changing environment.

In terms of signal transmission, past studies have shown that the response characteristic of test signal transmission is mainly related to signal frequency. And researches are concentrated on high speed and microwave circuits [3]. Signal transmission models can be established on the base of the telegraph operator equation [3]. Taking into account the solving complexity of the equation, a variety of numerical methods are widely developed from time domain or frequency domain. For example, finite different time domain method (FDTD) [4, 5], transmission line method (TLM) [6, 7], Inverse Fast Fourier Transform [8] (IFFT), numerical Laplace inverse transform method [9]

 Article number P_1307

(NLIT) and modal analysis method [10], were proposed to realize signal transmission analysis in specific conditions. Actually, signal transmission equation is the solution of circuit response. And then applying Spice-like equivalent circuit model, transient response analysis can be achieved by converting transmission parameters into pure circuit components [10]. These methods are valid for transmission network with high frequency distribution parameters, and can be also applied to analyze transient response of origin and terminal signal. However, the test signal of power system is different to microwave and high speed signal. The frequency of test signal is often mid or low frequency which is lower than that of high speed signal. And the transient response due to change of signal frequency is not obvious. So applying the previous methods to establish signal transmission model in high temperature environment has certain limitations.

In the paper, we cast the problem in change of signal response resulting from outer temperature field. Considering temperature-changing characteristic of transmission parameters, a new transmission model using FDTD is proposed to get test signal response changing with temperature. Corresponding experiment is carried out to prove the feasibility of simulation analysis.

2. Theory Model of Signal Transmission

The actual test signal is affected by many interfering factors. In the article, we only take change of ambient temperature as main influencing factor. First, the test signal network is given, shown as Fig. 1.

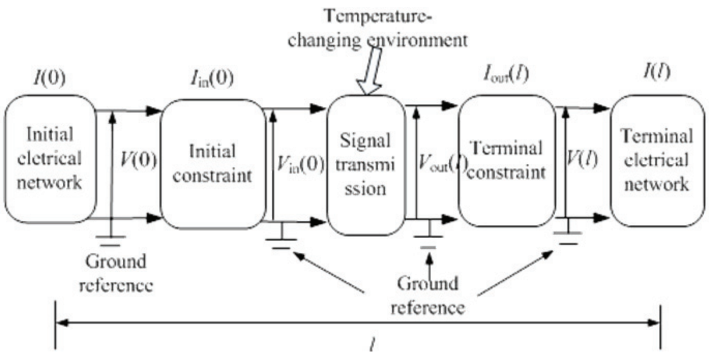

Fig. 1. Chart of test signal network.

In Fig. 1, $V(0)$ and $I(0)$ are input signals collected by the sensor, $V(l)$ and $I(l)$ are terminal signals. The transmission cable would change due to increase of ambient temperature.

When signal is transmitting in cable, the telegraph operator equation is satisfied for analyzing signal feature. The defined equation is followed

$$\begin{cases} \frac{\partial V}{\partial z} + \left(R + L\frac{\partial}{\partial t} \right) I = 0 \\ \frac{\partial I}{\partial z} + \left(G + C\frac{\partial}{\partial t} \right) V = 0 \end{cases} \tag{1}$$

Denote voltage V and current I in cable along the direction of z. Electric resistance R, electric capacity C and inductance L, electric conductance G are unit length transmission parameters of cable. From Eq. (1), it can be seen that no external input source is applied in signal transmission process. So, according to Fig. 1, it needs to put the signals collected by the sensor as input source, and new equation is obtained

$$\frac{\partial V(z,t)}{\partial t} + L\frac{\partial I(z,t)}{\partial t} + RI(z,t) = V_{\mathrm{F}}(z,t) \tag{2a}$$

$$\frac{\partial I(z,t)}{\partial t} + C\frac{\partial V(z,t)}{\partial t} + GV(z,t) = I_{\mathrm{F}}(z,t) \tag{2b}$$

Known from Eq. 2, $V(z,t), I(z,t)$ are related to time t. The $V_{\mathrm{F}}(z,t)$ and $I_{\mathrm{F}}(z,t)$ are the outside incentive source voltage and source current when time is t, corresponding to $V(0), I(0)$ in Fig. 1. In thermal environment, R, L, C, G are the function of temperature T. Substitute them into equations, and the Eq.2 becomes

$$\frac{\partial V(z,t)}{\partial t} + L(T)\frac{\partial I(z,t)}{\partial t} + R(T)I(z,t) = V_{\mathrm{F}}(z,t) \tag{3a}$$

$$\frac{\partial I(z,t)}{\partial t} + C(T)\frac{\partial V(z,t)}{\partial t} + G(T)V(z,t) = I_{\mathrm{F}}(z,t) \tag{3b}$$

,

Here, there are three parameters: t, z and T in transmission equation. So, it is more difficult to solve signal transmission equation than that with two parameters. According to the change of ambient temperature, a reasonable signal transmission model is given, and corresponding conversion method is presented using FDTD to realize iterative solution of signal transmission equation.

3. Model of Signal Transmission

Actually, the test environment is complex and diversified. So the temperature of selected environment is satisfied as Fig. 2.

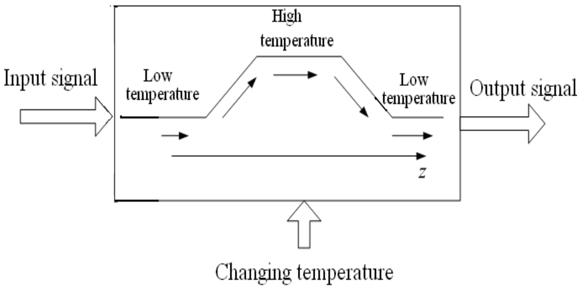

Fig. 2. Temperature gradient model.

Know from Fig. 2, to ensure the instrument work normally, the temperature in both ends of cable is low, setting as 20 ^{o}C. In the middle part, ambient temperature is high, more than 200 ^{o}C. Heat exchange results in change of cable temperature. The cable temperature is gradually changeable from low to high or from high to low.

3.1. Theoretical Model

For the signal transmission model shown as Fig. 2, transmission parameters have different values in different temperature. So, traditional integral method is hard to use to solve equation Eq. 3. On the basis of time and space discretization, temperature T is also discretized by the small load step to get a more precise result. Set $\triangle T$ as discrete temperature step. Now, parameters of R, L, C, G are expressed as $\triangle R(T)$, $\triangle L(T)$, $\triangle C(T)$, $\triangle G(T)$ in $\triangle T$ Then any part of is selected to analyze, and a transmission model with temperature gradient is shown in Fig. 3.

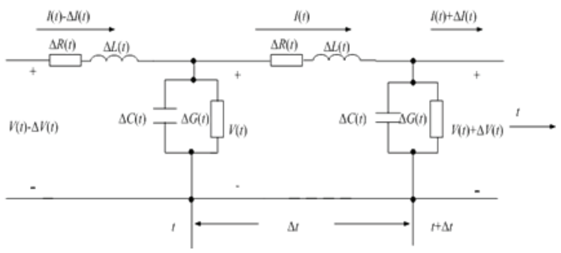

Fig. 3. Equivalent circuit diagram of temperature gradient model.

In Fig. 3, $V(T)$ and $I(T)$ are the initial voltage and current respectively, and $V(T)+\Delta V(T)$, $I(T)+\Delta I(T)$ are that at output ends. Applying Kirchhoff' s law in whole circuit, transmission equation Eq. (3) are converted as

$$\begin{aligned} &\frac{\partial V(T,t)}{\partial T} + R(T)\cdot I(T) + L(T)\frac{\partial I(T,t)}{\partial T} = V_F(T,t) \\ &\frac{dI(T,t)}{dT} + G(T)\cdot V(T) + C(T)\frac{\partial V(T,t)}{\partial T} = I_F(T,t), \end{aligned} \quad (4)$$

where, $V(T,t)$、$I(T,t)$ express the distribution of voltage and current when wire temperature is T in time t; $V_F(T,t)$, $I_F(T,t)$ are the outside incentive voltage and current source of unit length in time t. it is clear that the transmission equation of Eq.(4) contains two variables of time t and temperature T. So, it can be defined as temperature-time discrete model.

3.2. Iteration Solution

Applying partial ΔT section to the entire temperature field, the distribution of voltage and current are obtained by defined nodes, shown as Fig. 4. In charm of Fig. 4, only temperature and time are discrete representing as $\Delta T/2$ and $\Delta t/2$. And the voltage nodes and current nodes are cross-arranged, which the current node is in the middle of two voltage nodes.

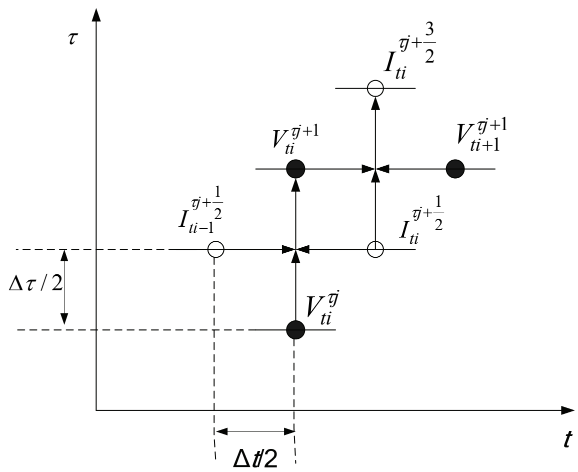

Fig. 4. Discrete chart of voltage and current on temperature and time.

Here, V_{Ti}^{tj} and I_{Ti}^{tj} are the voltage and current in different time and temperature respectively. Set V_{Ti}^{tj} and I_{Ti}^{tj} meet

$$\begin{aligned} V_{ti}^{\tau j} &= V((ti)\Delta t, j\Delta\tau) \\ I_{Ti}^{tj} &= I((Ti+1/2)\Delta t, j\Delta\tau) \end{aligned} \quad (5)$$

Then Eq. (4) can be obtained as follows

$$\frac{V_{ti+1}^{\tau j+1}-V_{ti}^{\tau j+1}}{\Delta t}+L_{ti}\cdot\frac{I_{ti}^{\tau j+\frac{3}{2}}-I_{ti}^{\tau j+\frac{1}{2}}}{\Delta\tau}+R_{ti}\cdot\frac{I_{ti}^{\tau j+\frac{3}{2}}+I_{ti}^{\tau j+\frac{1}{2}}}{2}=\frac{V_{\mathrm{F}}^{\tau j+\frac{3}{2}}+V_{\mathrm{F}}^{\tau j+\frac{1}{2}}}{2}$$

$$\frac{I_{ti}^{\tau j+\frac{1}{2}}-I_{ti-1}^{\tau j+\frac{1}{2}}}{\Delta t}+G_{ti}\cdot\frac{V_{ti}^{\tau j+1}-V_{ti-1}^{\tau j}}{\Delta\tau}+C_{ti}\cdot\frac{V_{ti}^{\tau j+1}+V_{ti}^{\tau j}}{2}=\frac{I_{\mathrm{F}}^{\tau j+1}+I_{\mathrm{F}}^{\tau j}}{2} \tag{6}$$

The further organization is carried out for formula, and we have

$$\left(L_{ti}\frac{\Delta t}{\Delta\tau}+\frac{R_{ti}}{2}\Delta t\right)I_{ti}^{\tau j+\frac{3}{2}}=\left(L_{ti}\frac{\Delta t}{\Delta\tau}-\frac{R_{ti}}{2}\Delta t\right)I_{ti}^{\tau j+\frac{1}{2}}-\left(V_{ti+1}^{\tau j+1}-V_{ti}^{\tau j+1}\right)+\frac{\Delta t}{2}\left(V_{\mathrm{F}}^{\tau j+\frac{3}{2}}+V_{\mathrm{F}}^{\tau j+\frac{1}{2}}\right) \tag{7a}$$

$$\left(C_{ti}\frac{\Delta t}{\Delta\tau}+\frac{G_{ti}}{2}\Delta t\right)V_{ti}^{\tau j+1}=\left(C_{ti}\frac{\Delta t}{\Delta\tau}-\frac{G_{ti}}{2}\Delta t\right)V_{ti}^{\tau j}-\left(I_{ti}^{\tau j+\frac{1}{2}}-I_{ti-1}^{\tau j+\frac{1}{2}}\right)+\frac{\Delta t}{2}\left(I_{F}^{\tau j+1}+I_{F}^{\tau j}\right) \tag{7b}$$

3.3. The Initial and Boundary Conditions

Known from Fig. 3, the Initial conditions of signal transmission meet T_1=T_0, and there is a source matched resistance R_{S}, so conditions meet

$$G_{t0}=\frac{1}{R_{\mathrm{S}}} \tag{8a}$$

$$\frac{C_{t0}}{2}\Delta t=C_{ti}\Delta t \tag{8b}$$

$$I_{\mathrm{F}}=\frac{V_{\mathrm{S}}}{R_{\mathrm{S}}\Delta t} \tag{8c}$$

Taking the boundary condition Eq. (8) into Eq. (7a), Voltage and current can be expressed at T_1 °C

$$\left(C_{t0}R_{\mathrm{S}}\frac{\Delta t}{\Delta\tau}+1\right)V_{t1}^{\tau j+1}=\left(C_{t0}R_{\mathrm{S}}\frac{\Delta t}{\Delta\tau}-1\right)V_{t1}^{\tau j}-2R_{\mathrm{S}}I_{t1}^{\tau j+\frac{1}{2}}+\left(V_{\mathrm{S}}^{\tau j+1}+V_{\mathrm{S}}^{\tau j}\right) \tag{9}$$

When the matched resistance R_{L} is at T_{N+1}°C, the boundary conditions becomes

$$I_{\mathrm{tN+1}}=0 \tag{10a}$$

$$G_{\mathrm{tN+1}}\Delta t=\frac{1}{R_{\mathrm{L}}} \tag{10b}$$

$$I_{\mathrm{F}}\Delta t=\frac{V_{\mathrm{L}}}{R_{\mathrm{L}}} \tag{10c}$$

$$\frac{C_{\mathrm{L}}}{2}\Delta t=C_{\mathrm{T}i}\Delta t \tag{10d}$$

By Eq. (7b) and Eq. (10), the equation at T_{N+1}°C can be solved as followed formula.

$$\left(C_{tN}R_{\mathrm{L}}\frac{\Delta t}{\Delta\tau}+1\right)V_{tN+1}^{\tau j+1}=\left(C_{tN}R_{\mathrm{L}}\frac{\Delta t}{\Delta\tau}-1\right)V_{tN+1}^{\tau j}+2R_{\mathrm{L}}I_{tN}^{\tau j+\frac{1}{2}}+\left(V_{\mathrm{L}}^{\tau j+1}+V_{\mathrm{L}}^{\tau j}\right) \tag{11}$$

3.4. Iterative Algorithm Based on Temperature-time

Form T_2 °C to T_N °C, there is no external excitation acting on wire, with V_{F} =0 and I_{F}=0. Applying initial condition of Eq. (8) and boundary conditions of Eq. (9), the discrete iterative equations of signal transmission are given as follows

$$V_{t1}^{\tau j+1}=\left(C_{t0}R_S\frac{\Delta t}{\Delta\tau}+1\right)^{-1}\left\{\left(C_{t0}R_S\frac{\Delta t}{\Delta\tau}-1\right)V_{t1}^{\tau j}-2R_SI_{t1}^{tj+\frac{1}{2}}+\left(V_S^{\tau j+1}+V_S^{\tau j}\right)\right\} \tag{12a}$$

$$V_{tN+1}^{\tau j+1}=\left(C_{tN}R_{\mathrm{L}}\frac{\Delta t}{\Delta\tau}+1\right)^{-1}\left\{\left(C_{tN}R_{\mathrm{L}}\frac{\Delta t}{\Delta\tau}-1\right)V_{tN+1}^{\tau j}+2R_{\mathrm{L}}I\tau_{tN}^{tj+\frac{1}{2}}+\left(V_{\mathrm{L}}^{\tau j+1}+V_{\mathrm{L}}^{\tau j}\right)\right\} \tag{12b}$$

$$V_{ti}^{\tau j+1}=\left(C_{ti-1}\frac{\Delta t}{\Delta\tau}+\frac{G_{ti-1}}{2}\Delta t\right)^{-1}\left\{\left(C_{ti-1}\frac{\Delta t}{\Delta\tau}-\frac{G_{ti-1}}{2}\Delta t\right)V_{ti}^{\tau j}-\left(I_{ti}^{\tau j+\frac{1}{2}}-I_{ti-1}^{\tau j+\frac{1}{2}}\right)\right\} \tag{12c}$$

$$I_{ti}^{tj+1/2}=\left(L_{ti}\frac{\Delta t}{\Delta\tau}+\frac{R_{ti}}{2}\Delta t\right)^{-1}\left\{\left(L_{ti}\frac{\Delta t}{\Delta\tau}-\frac{R_{ti-1}}{2}\Delta t\right)I_{ti}^{\tau j-\frac{1}{2}}-\left(V_{ti+1}^{\tau j}-V_{ti}^{\tau j}\right)\right\} \tag{12d}$$

To ensure the astringency of iterative equations, the ΔT and Δt are small enough to get a good precision of solution. In Eq. (12), not only R, L, C and G are related to temperature, but also the voltage and current change with increase of temperature. Thus, compared to equation with constant parameters, it is harder for the solution of Eq. (12).

4. Simulation Analysis

According to Fig. 2, a signal transmission model is established, shown in Fig. 5. In the circuit, the temperature change of cable is obvious from T_0 to T_{max} and from T_{max} to T_0.

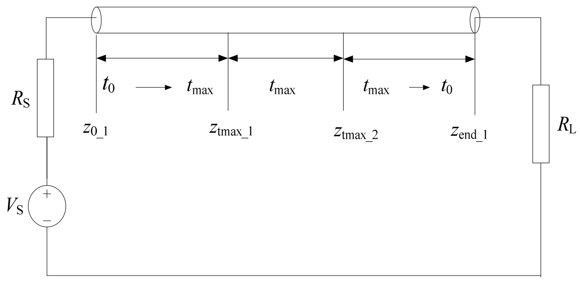

Fig. 5. Signal transmission model changing with temperature.

Here, Vs is the signal input source; Rs and R_L are initial and terminal resistance respectively; z_{0_1} is start point of cable with temperature of T_0 °C; z_{Tmax_1} and z_{Tmax_2} are the position corresponding to temperature of T_{max} °C ; z_{end_1} is terminal point of cable with temperature reduced to T_0°C. In whole test process, high temperature coaxial-cable is applied for signal transmission. The corresponding parameters characteristics of RLCG are referred in reference [11]. It can be seen from Fig. 5, the transmission network of test signal is composed of three parts: temperature rise of cable along direction of z, maintained at high temperature and temperature drop of cable along direction of z. Here the above three process can be solved respectively, and the total signal response is also able to analyzed.

4.1. Change of Signal Amplitude

To avoid signal delay caused by too long cable, the length of transmission wire is set as 10 m. The input signal at z_{0_1} is sinusoidal signal with amplitude of 1 V and frequency of 1000 Hz. The signal is collected at $z_{end\_1.}$ Initial resistance R_S is equal to terminal and R_L, which are 50 Ω. The circuit satisfies impedance matching, and magnitude of output signal is half of that of input signal.

In the paper, initial temperature of the wire is 20 °C, and the maximum of temperature is 300 °C. Applying all the conditions, iterative equation of Eq. (12) is solved by Matlab programming. First, feature of signal transmission at single temperature environment is discussed, and Fig. 6 shows the comparison of signal response at 30 °C and 300 °C.

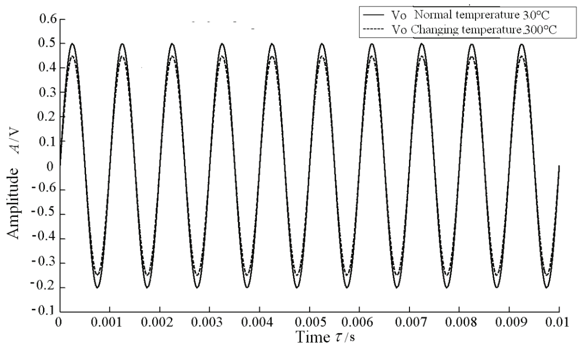

Fig. 6. Signal response of 1000 Hz at 20 °C and 100 °C.

As shown by the Fig. 6, the change of temperatures puts an important influence on signal output response Vo. Here, the solid and dashed lines show the output response at 30 °C and 300 °C separately. It can be observed that amplitude of signal response at 300 °C drops significantly, reached to 95.036 % of that at 30 °C. From the results, it can be demonstrated that temperature effect for output signal can be not ignored. And the reason of amplitude reducing is mainly from temperature-changing characteristic of RLCG. Compared to amplitude, phase deviation of signal is smaller effected by temperature variation. Therefore, we will put main attention to analyze change of signal amplitude caused by temperature rise or drop.

4.2. Amplitude Change at Different Temperature

In test environment of Fig. 5, change of cable temperature is composed of three processes successively. The obtained signal response is consistent with the above processes. Detailed analysis is given below.

1) Temperature rise of transmission path: As can be seen that the temperature of cable keeps constant of 30 °C from 0 to z_{0-1}, and temperature increases gradually from 30°C to 300 °C in part of z_{0-1}~z_{Tmax-1}.
2) Temperature decrease: In part of z_{Tmax-2}~z_{end-1}, temperature of cable decreases from high to constant, that is 300 °C at z_{Tmax-2} and 30 °C at z_{end-1}. It is worth noting that input signal at z_{Tmax-2} is considered as same to that of temperature rise process.
3) Temperature rise-constant-decrease: The exact model meeting to original model of Fig. 5 is composed of temperature rise, decrease and the middle part with high temperature. Firstly, the attenuation of signal transmission is taken place due to rise of temperature. Because transmission

parameters remain constant at a certain temperature, it can be considered the signal transmission without attenuation from z_{Tmax-1} to z_{Tmax-2}. And then, the initial input signal in temperature decrease process is not same to that of temperature rise process, but is the signal of temperature rise after attenuation.

To discuss signal response at different T_{max}, we take T_{max} as a set of temperature vector arranged from low to high. And then, V_{o_T} is set as amplitude of signal response at T_{max}, and V_{o_30} is output signal at 30 °C. To obtain more comparison of response δ_T is defined as the percentage of signal amplitude, following as

$$\delta_T = \left(1 - \frac{V_{o\_T}}{V_{o\_30}}\right) \times 100\% \tag{13}$$

Therefore, the attenuation of signal response can be represented using δ_T , and Table 1 provides the attenuate values in three processes at different temperature.

Table 1. Comparison of signal response attenuation at different process.

T_{max} (°C)	30	50	100	150	200	250	300
δ_T at temperature rise /%	0.13	0.59	1.45	2.32	3.16	4.00	4.96
δ_T at temperature decrease /%	0.09	0.56	1.41	2.28	3.12	3.96	4.92
δ_T at total process /%	0.26	1.17	2.84	4.55	6.18	7.8	9.65

It can be seen from Table 1, the attenuate degree of δ_T is approximately same in processes of temperature rise and decrease. When ambient temperature is below 50 °C, the signal attenuation is small and can be ignored. However, the attenuate amplitude becomes accretive gradually over 100 °C, with the attenuate of 5 % at 300 °C comparing to room temperature. Taking into account transmission parameters remain unchanged in thermostat stage, test signal is considered as no attenuate transmission. Here, output signal of temperature rise process becomes the input signal of temperature decrease process, which would result in the greater attenuation of signal. In Table 1, the attenuation of signal is proportional to temperature rise, and the higher the temperature is, the greater the attenuation of signal. Especially at 300 °C, signal amplitude is only 90 % of that at 30 °C, reduced by 10 %. So, when ambient temperature is over 100 °C, the attenuation of signal amplitude should be taken seriously enough. It also shows that it is undoubtedly indeterminate to judge the structural feature using such signal.

5. Experiment in Temperature Changing Environment

In fact, the influence of environmental temperature on test signal is achieved through the effect of temperature on the wire. The experiment is carried out on the basis of test bench of vibration test. The impact of temperature on signal is analyzed by measuring the structural vibration parameters and heating wire locally.

5.1. Experiment System

The experiment system is composed of three components: vibration test system, environmental temperature changing system and data acquisition and processing system. In vibration testing system, choose the steel plate as experiment component, and acceleration transducer is applied to test and output two signals. In temperature changing part, the wires are placed in iron drum, and adjustable electric furnace is used to heat wires to make temperature rise, shown as Fig. 7.

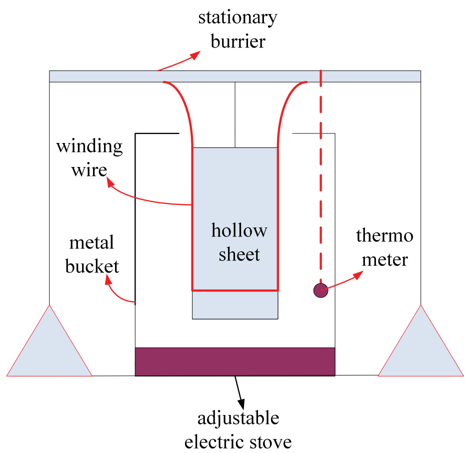

Fig. 7. Test of temperature changing environment.

It is shown from Fig. 7 that temperature of red horizontal wires is at the highest temperature. Moreover, temperature of surrounding wire reduces gradually due to barrel heat dissipation from low to high. The temperature-changing process is good meet to the analytical model. The specific experimental procedure is as follows.

First, open the adjustable electric furnace and keep it at certain power. Test the ambient temperature constantly, until the thermometer Index is constant. Start the vibration test system. Keeping the signal power amplification constant, two signals are obtained: the original signal 1 of no temperature impact and test signal 2 influenced by ambient temperature. All the data is collected and recorded by computer.

5.2. Analysis of Experiment Data

It is worth noting that adjusting the electric power can cause temperature change of the barrel, which would also generate different highest temperature of the wires. Considering the effect from noise signal, the collected signal is filtered by proper band-pass and band-stop filter. The output signals of 100 Hz at different temperature are shown in Fig. 8.

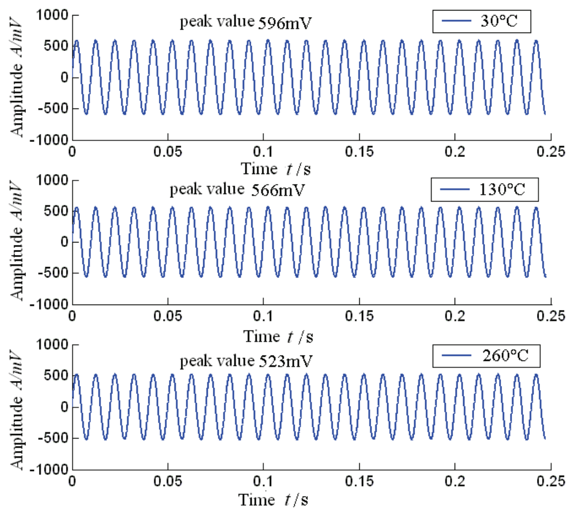

Fig. 8. Signal response after filter at different temperature.

Here, ambient temperature is set to 30 °C. The results from Fig. 8 show that average amplitude of output signal is reduced from 596 mV at 30 °C to 523 mV at 260 °C, with the attenuation degree of 12.25 %. It also indicates that average amplitude of signal is gradually reduced with temperature rise.

The simulation analysis results and the test results were compared using the above-mentioned principle, and then the change results while it is 1000 Hz were shown in Fig. 9.

In experiment, different signals at several temperatures are compared to deeply discuss temperature influence on signal amplitude. Same as above, ambient temperature is 30 °C as a reference, and the amplitude percentage of δ_t is used to represent signal change. When the signal frequency is 1000 Hz, all the experiment and simulation results can be shown using Fig. 9.

As can be seen from the Fig. 9, the amplitude variation obtained by simulation is approximately linear distribution, and is inversely proportional to temperature change. Relatively speaking, the experimental results are fluctuated within a certain range. The reason is believed that only a single signal transmits in the wire ignoring other interference signal in simulation analysis, which is an ideal case analysis. In actual test process, certain error is evitable in experiment. And it is more difficult to completely eliminate effect of interference signal by filtering and other technology. Although, the relationship between signal and temperature is very clear and is nearly consistent with simulation results. At 260 °C, the average amplitude of simulation and experimental results are respectively 91.99 % and 87.75 % of that at 30 °C. Relatively, experimental results changes significantly and signal amplitude has a greater attenuation than simulation results.

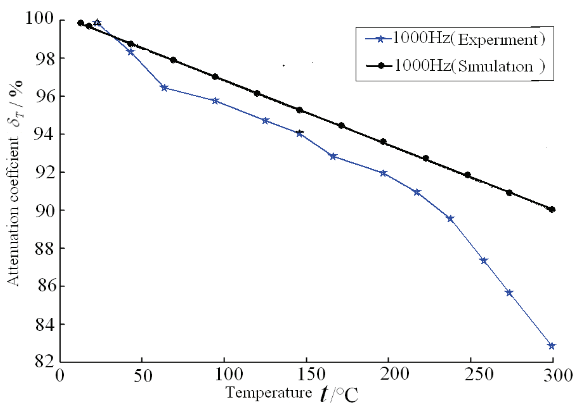

Fig. 9. Experiment and simulation results.

6. Conclusions

For the general vibration testing system, the influence, such as ambient temperature, is often ignored. And if considering temperature, it is also hard to get the specific influence of temperature variation on signal response using conventional signal processing method. In the paper, the FDTD method is successfully applied to achieve the simulation analysis, and corresponding experimental test is carried in temperature changing environment. Firstly, a circuit network is established to express signal transmission part of vibration testing system visually. Applying the temperature-changing characteristics of RLCG parameters, a new approach based on FDTD is proposed to create iteration equations. A transmission model with temperature rise and decrease is given using simulation analysis. From simulation results, we can found that signal amplitude doesn't keep unchanged in whole process. Signal amplitude has a greater attenuation in above temperature change process. The higher the temperature is, the more attenuate the signal amplitude has. When reach to 300 °C, the signal amplitude is only about 90 % of that at 30 °C. This is fully shown that characteristic of original signal has changed from energy point. In the paper, corresponding experiment is given and it has same temperature characteristic to simulation. By using conduction of heat, temperature of wire increases and decreases gradually in test experiment. The signal feature changing with temperature is consistent both in simulation and experimental results. Therefore, it is better to improve the precision of signal analysis when considering the influence of ambient temperature to signal.

Acknowledgements

This research was supported by Shan Dong Scientific Research Foundation for Excellent Young Scientists (Grant No: BS2011ZZ001), National Natural Science Foundation of China (Grant No. 51105172) and National Natural Science Foundation of China (Grant No.51205165).

References

[1]. Liao Qingbin, Li Shunming, Qin Xiaopan, Comparison of feature extraction methods of vehicle vibration signal, *Journal of Jilin University, Engineering and Technology Edition*, 37, 4, 2007, pp. 910-9144.

[2]. Sun Qiang, Zhang Zhongpin, Chai Qiao et al., Temperature effect on vibration frequency of aero-engine compressor blade, *Chinese Journal of Applied Mechanics,* 2004, 21, 4, pp. 137-139.

[3]. Antonije R. D., Sarkar T. K., Harrington R F., Time-domain response of multiconductor transmission lines, *Proceeding of the IEEE*, 75, 6, 1987, pp. 743-764.

[4]. Ruehli A. E., Cangellaris A. C., Progress in the methodologies for the electrical modeling of interconnects and electronic packages, in *Proceedings of the IEEE*, 89, 5, 2001, pp. 740-771.

[5]. Antonini G., Antonio O., Clayton R. P., An improved method of modeling lossy transmission lines finite-difference time-domain analysis, in Proceedings of the *IEEE International Symposium on Electromagnetic Compatibility,* 1999, pp. 435-439.

[6]. Wolfgang J. R., The transmission linematrix method-theory and applications, *IEEE Trans. on MTT*, 33, 10, 1985, pp. 882-893.

[7]. Lau F. Waveform relaxation analysis of lossy coupled transmission line sets in cascade, *IEEE Proc-Circuits Devices Systems,* 142, 6, 1995, pp. 373-378.

[8]. Guo Yushun, Transmission line model of transient simulation derived using the NLIT technique, *Acta Electronic Sinica*, 30, 3, 2002, pp. 381-385.

[9]. Sergio G., Martins N., Sergio L. V., et al., Modal analysis of electromagnetic transients in ac networks having long transmission lines, *IEEE Trans. Power Del.,* 20, 4, 2005, pp. 2623-2630.

[10]. Caniggia S., Maradei F., Spice-like models for the analysis of the conducted and radiated immunity of shielded cables, *IEEE Trans. Electromagn. Compat.,* 43, 4, 2004, pp. 606-616.

[11]. Men Xiuhua, Li Shunming, Hu Rui, et. al., Effects on transmission parameters of vibration measurement for high temperature environment, *Journal of Aerospace Power,* 24, 9, 2009, pp. 1731-1735.